

Impedance Matching Design of Small Normal Mode Helical Antennas for RFID Tags

Yi Liao, Yuan Zhang, Kun Cai, and Zichang Liang

Shanghai Key Laboratory of Electromagnetic Environmental Effects for Aerospace Vehicle

No. 846 Minjing RD

Yangpu District, Shanghai 200438 China

Abstract—The normal mode helical antenna (NMHA) is widely used on RFID applications because it fits well with the requirements of smaller physical size and high inductive impedance. In this paper, a power transmission coefficient method of mapping a modified impedance function onto the conventional Smith chart is applied to conjugate matching design between NMHA and chips. Moreover, the effect of various geometrical parameters of NMHA on resonant frequency and input impedance is investigated. Some significant characteristics of NMHA in the Smith chart are obtained by varying each parameter. It could provide an effective guidance to tune the antenna to desirable complex impedance in the Smith chart. Finally, impedance matching design of a specific NMHA is conducted according to the previously mentioned method.

I. INTRODUCTION

The normal mode helical antenna (NMHA) is the kind of helical antenna with the circumference of helix much smaller than a wavelength [1]. The radiation pattern of NMHA is generally similar to that of the dipole antenna and the physical size, with its self resonant structure, is much shorter compared to the dipole antenna [2]. It is even electrically smaller when placed in a dielectric medium. Therefore, the NMHA is widely used for many RF identification (RFID) applications such as portable equipments, TPMS in vehicles, and access control [3]-[5].

A typical RFID tag consists of an antenna and a chip whose impedance is strongly capacitive. Most of the available RFID chips in the ultra-high-frequency (UHF) band exhibit a reactance roughly ranging from -100Ω to -600Ω , while the real part is much smaller [6]. Generally, conjugate matching is achieved between antenna and chip for maximum power transfer [7]. A very straightforward way for impedance matching is to use the Smith chart which is usually normalized to 50Ω . Nevertheless, a method where modified impedance function is mapped onto the conventional Smith chart to determine a power transmission coefficient is much more convenient for the case when both generator and load impedances are complex [8].

Although helical antennas have been known for more than half a century, it seems that reliable formulae for helical antennas do not exist in the open literature [9]. Therefore, numerical tools are essential to helical antenna design and analysis [10]. Resonant frequency and impedance characteristics of NMHA are the functions of its various physical parameters. This paper uses a full-wave numerical

modeling tool to calculate the resonant frequency and the input impedance of NMHA [11]. The impedances are mapped onto the Smith Chart based on the power transmission coefficient method. The results are analyzed by varying one parameter each time. The purpose is to investigate how these parameters influence the resonant frequency and input impedance of NMHA. It helps to give a significant guidance for NMHA design to achieve the inductive input reactance required for the microchip conjugate impedance matching in practical cases.

II. IMPEDANCE MATCHING FOR NMHA

A. Power transmission coefficient method

In passive RFID tags, the chip is usually directly connected to the input terminals of the tag antenna and both the chip and antenna have complex input impedances. An equivalent circuit is shown in Fig. 1, which represents the RFID tag in the receiving mode.

V_S is the equivalent voltage source in the antenna port, $Z_A = R_A + jX_A$ is the antenna impedance, $Z_L = R_L + jX_L$ is the chip impedance. The reflection coefficient can be expressed by

$$\Gamma = \frac{Z_L - Z_A^*}{Z_L + Z_A^*}. \quad (1)$$

And the power transmission coefficient

$$\sigma = 1 - |\Gamma|^2 = \frac{|Z_L - Z_A^*|^2}{|Z_L + Z_A^*|^2}. \quad (2)$$

It shows what fraction of the maximum power available from the generator is delivered to the load and determines the read distance of the RFID device.

Kurokawa described a graphically intuitive way to obtain the reflection coefficient Γ plotted in the Smith chart [12]. It makes a transformation to move the Z_L to the center of the Smith chart by using the normalized impedance

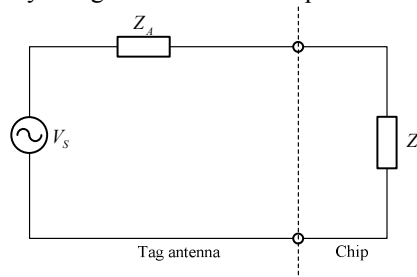


Figure 1. Equivalent circuit for RFID tag.

$$r + jx = \frac{R_A}{R_L} + j \frac{X_A + X_L}{R_L}. \quad (3)$$

The contours of constant reflection coefficient are concentric circles centered around the origin of the Smith chart, which corresponds to a perfect complex conjugate match. Therefore, the power transmission coefficient σ can be easily calculated from the Smith chart.

B. NMHA impedance in the normalized Smith chart

Fig.1 shows the geometry of a typical helical dipole antenna. The helix is uniformly wound with a constant pitch, S . The diameter of a helix is D . The helix's conductor is a wire of radius, a . The antenna is fed at the midpoint of the coil winding with a constant diameter, and uniform circular cross section of the conductor.

In this section, three parameters, N , S , and D are considered. The geometrical parameters of the antennas grouped in three sets are given in Table 1. Resonant frequencies, as well as the input impedances over the frequency range from resonance to antiresonance in the Smith chart are presented when one of physical parameters is varied. All the impedances shown in Smith Chart are normalized with the reference impedance of $50-j50 \Omega$. The analysis frequency range is from 700 MHz to 1400 MHz, which covers the UHF RFID bands.

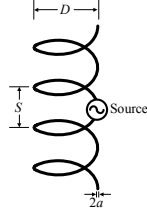


Figure 2. A typical helical dipole antenna.

TABLE I
GEOMETRICAL PARAMETERS OF NMHA

No	Geometry ($a=0.1$ mm)	Resonant Frequency
Different number of turns		
1	$D=1.2$ mm, $S=0.7$ mm, $N=110$ turns	846 MHz
2	$D=1.2$ mm, $S=0.7$ mm, $N=115$ turns	813 MHz
3	$D=1.2$ mm, $S=0.7$ mm, $N=120$ turns	783 MHz
4	$D=1.2$ mm, $S=0.7$ mm, $N=125$ turns	756 MHz
5	$D=1.2$ mm, $S=0.7$ mm, $N=130$ turns	730 MHz
Different pitch		
6	$D=1.2$ mm, $N=120$ turns, $S=0.5$ mm	827 MHz
7	$D=1.2$ mm, $N=120$ turns, $S=0.6$ mm	809 MHz
8	$D=1.2$ mm, $N=120$ turns, $S=0.7$ mm	783 MHz
9	$D=1.2$ mm, $N=120$ turns, $S=0.8$ mm	755 MHz
10	$D=1.2$ mm, $N=120$ turns, $S=0.9$ mm	725 MHz
Different diameter		
11	$S=0.7$ mm, $N=120$ turns, $D=1.10$ mm	851 MHz
12	$S=0.7$ mm, $N=120$ turns, $D=1.15$ mm	816 MHz
13	$S=0.7$ mm, $N=120$ turns, $D=1.20$ mm	783 MHz
14	$S=0.7$ mm, $N=120$ turns, $D=1.25$ mm	752 MHz
15	$S=0.7$ mm, $N=120$ turns, $D=1.30$ mm	724 MHz

The number of turns varies from 110 to 130 with an interval of 5 as shown in Table 1. As the number of turns increases the resonant frequency decreases. Fig. 3 indicates that two input impedance locus curves are almost the same in the Smith Chart. Basically, changing the number of turns will not influence the input impedance locus in a significant way as long as N exceeds a critical number [13].

When pitch is varied from 0.5 mm to 0.9 mm the resonant frequency decreases. Fig. 4 depicts two impedance curves for case 6 and case 10. The dashed curve ($S=0.5$ mm) moves outwards to the unity cycle in the Smith Chart. It also indicates that smaller pitch of the antenna has the smaller resistance at resonant frequency.

The increasing diameter lowers the resonant frequency as shown in Table 1. Fig. 5 gives the results when varying D . The input impedance is very sensitive to the helix diameter, the dashed curve moves inwards as D increasing.

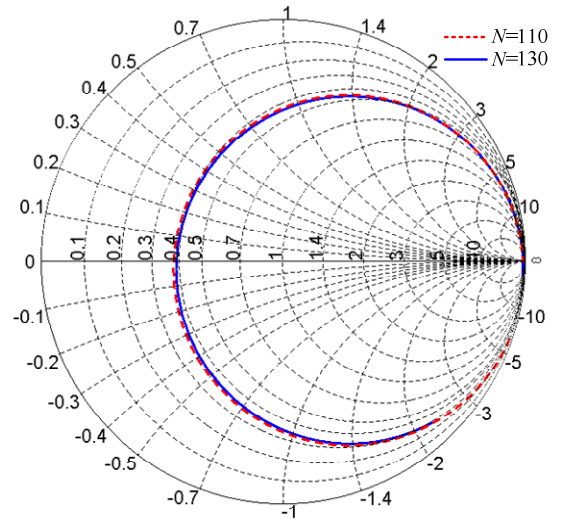


Figure 3. NMHA input impedance mapped onto the Smith chart normalized to $50-j50 \Omega$ for case 1(dashed curve) and case 5 (solid curve).

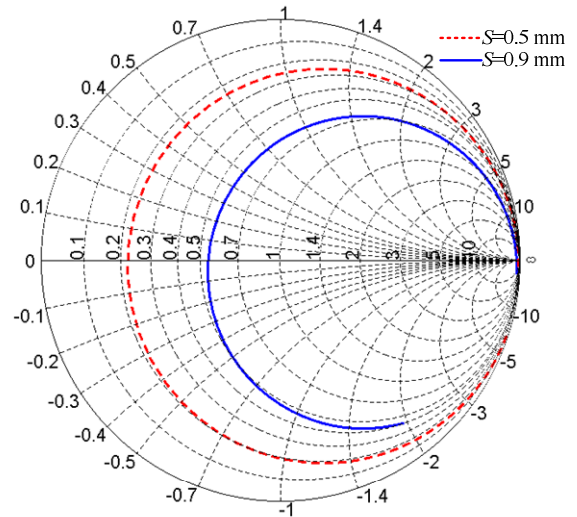


Figure 4. NMHA input impedance mapped onto the Smith chart normalized to $50-j50 \Omega$ for case 6(dashed curve) and case 10 (solid curve).

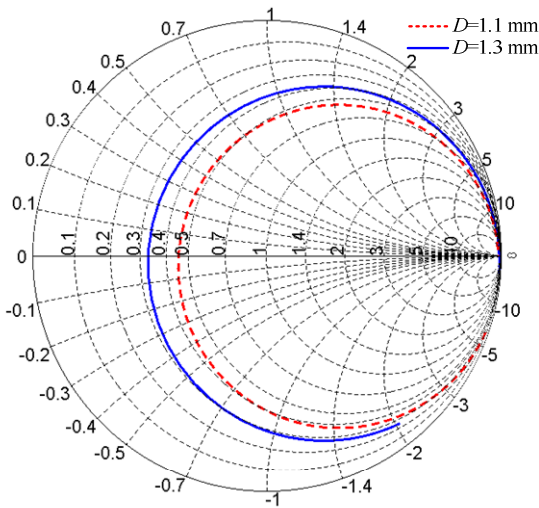


Figure 5. NMHA input impedance mapped onto the Smith chart normalized to $50-j50 \Omega$ for case 11 (dashed curve) and case 15 (solid curve).

It can be seen that the behaviors of impedance in the Smith chart are regular within a certain range for each parameter. It is very convenient to get the desired resonant frequency and impedance by changing geometrical parameters for small normal mode helical antennas.

III. IMPEDANCE MATCHING DESIGN EXAMPLE

Since every chip for RFID tag has complex impedance and there is no consistency for different manufactures, designers usually have to adjust the impedance to realize conjugate matching with chip complex impedance to maximize antenna performance. As an example, consider a UHF tag designed for tire pressure monitoring system (TPMS) in vehicle. The tag employs a normal mode helical antenna embedded in a dielectric block with the dimensions of $100 \times 20 \times 20 \text{ mm}^3$ and relative permittivity of 5. The impedance of RFID chip is $Z_L = 27-j201 \Omega$, approximately constant in the frequency range of interest (902 MHz ~ 928 MHz).

Fig.6 shows the geometry of NMHA in a dielectric block. For clarity, only a limited number of helix coils are illustrated. A 3-mm straight wire is used in the middle to directly connect the antenna with the chip. Let us start with the initial parameters: $a=0.1 \text{ mm}$, $D=1.1 \text{ mm}$, $S=0.6 \text{ mm}$, $N=80$.

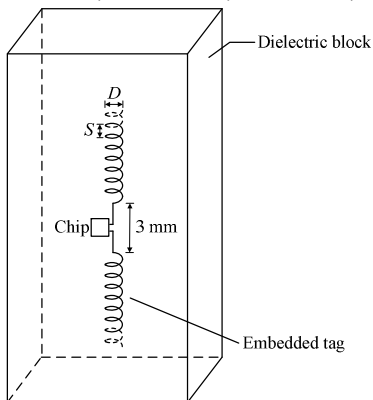


Figure 6. NMHA embedded in the dielectric block.

Fig. 7 shows the frequency-dependent NMHA impedance mapped onto the Smith chart normalized to $27-j201 \Omega$. Locus (a) is the impedance of initial geometry of NMHA over the frequency range from 660 MHz to 1060 MHz. The reflection coefficient within the considered bands (902 MHz ~ 928 MHz) is far away from the origin of the Smith chart ($|\Gamma| \approx 1$).

For the sake of achieving the conjugate match, we have to adjust the geometrical parameters to make the impedance locus curve move closer to the center of Smith chart. Since the important information we obtain previously is that the impedance locus is not sensitive to the number of turns, the parameters D and S are firstly adjusted to make the NMHA impedance locus move inward and go through the origin of the Smith chart. Then the helices are cut shorter uniformly in two sides of NMHA to obtain the tag resonant frequency and impedance matching. Locus (b) in Fig.7 describes the results of final NMHA with the geometrical parameters: $a=0.1 \text{ mm}$, $D=1 \text{ mm}$, $S=0.785 \text{ mm}$, $N=69$.

The power transmission coefficient over the frequency range of interest (902 MHz~928 MHz) is also calculated from the Smith chart by observing the distance between the origin and the mapped impedance point, as shown in Fig.8. It can be seen that conjugate matching is achieved around 915 MHz where the maximum σ is obtained.

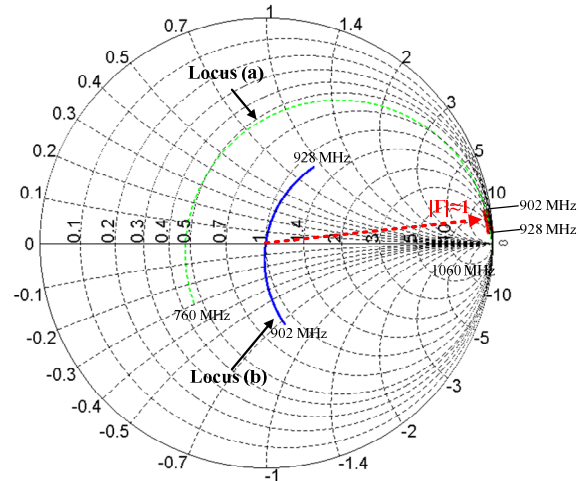


Figure 7. Impedance mapped onto the Smith chart normalized to $27-j201 \Omega$ for matching design.

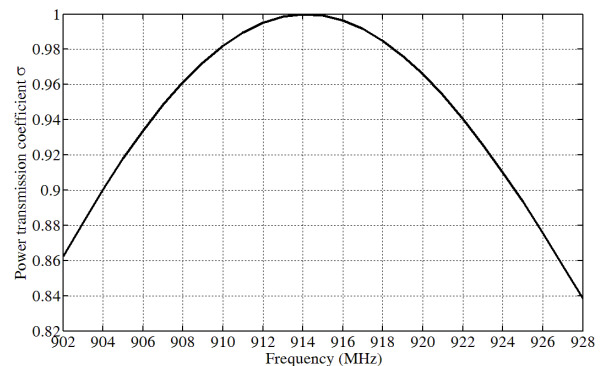


Figure 8. Power transmission coefficient σ versus frequency.

IV. CONCLUSION

Small normal mode helical antennas are usually directly connected to the chip in RFID tags due to cost and fabrication issues. In this paper, a power transmission coefficient method is employed to get conjugate impedance matching in the Smith chart for NMHA. The resonant frequency and impedance characteristics of NMHA depending on the configuration of the physical parameters are also investigated. Three parameters are considered. It helps to provide effective guidance for designers to tune the impedance of NMHA to desirable value in the Smith chart. Finally, a specific NMHA is given and demonstrated for impedance matching design.

REFERENCES

- [1] J. D. Kraus, *Antennas*, 2nd ed., New York: McGraw-Hill, 1988, pp. 274-276.
- [2] Y. Hiroi and K. Fujimoto, "Practical usefulness of normal helical antenna," *IEEE AP-S Int. Symp.*, pp. 238-241, 1976.
- [3] H. Morishita, Y. Kim, H. Furuuchi, K. Sugita, Z. Tanaka, et al., "Small balance-fed helical dipole antenna system for handset," *51st IEEE Vehicular Technology Conference Proc.*, Toyko, vol. 2, pp. 1377-1380, May 2000.
- [4] N. Q. Dinh, N. Michishita, Y. Yamada, and K. Nakatani, "Electrical characteristics of a very small normal mode helical antenna mounted on a wheel in the TPMS application," *IEEE AP-S Int. Symp.*, pp. 1-4, 2009.
- [5] Y. Yamada, W. G. Hong, W. H. Jung, and N. Michishita, "High gain design of a very small normal mode helical antenna for RFID tags," *IEEE Region 10 Conference*, pp.1-4, 2007.
- [6] G. Marrocco, "The art of UHF RFID antenna design: impedance-matching and size-reduction techniques," *IEEE Antennas and Propagation Magazine*, vol. 50, no. 1, pp. 66-79, February 2008.
- [7] K. V. S. Rao, P. V. Nikitin, and S. F. Lam, "Impedance matching concepts in RFID transponder design," *4th IEEE Automat. Identification Adv. Technol. Workshop*, pp. 39-42, October 2005.
- [8] P. V. Nikitin, K. V. S. Rao, S. F. Lam, V. Pillai, R. Martinez, et al., "Power reflection coefficient analysis for complex impedances in RFID tag design," *IEEE Trans. on Microw. Theory and Techn.*, vol. 53, no. 9, September 2005.
- [9] A. R. Djordjevic, A. G. Zajic, M. M. Ilic, and G. L. Stuber, "Optimization of helical antennas," *IEEE Trans. on Antennas and Propagation*, vol. 46, pp. 525-530, 1998.
- [10] C. Su, H. Ke, and T. H. Hubing, "A simplified model for normal mode helical antennas," *ACES Journal*, vol. 25, no. 1, pp.32-40, January 2010.
- [11] "FEKO User's Manual," EM Software & Systems-S.A. (Pty) Ltd, 32 Techno Avenue, Technopark, Stellenbosch, 7600, South Africa, 2011.
- [12] K. Kurokawa, "Power waves and the scattering matrix," *IEEE Trans. Microw. Theory Tech.*, vol. MTT-13, no. 3, pp. 194-202, March 1965.
- [13] K. H. Awadalla, S. H. Zainud-Deen, and H. A. Sharsher, "Analysis of normal mode helical antenna and scatterer", *IEEE AP-S Int. Symp.*, pp. 1731-1734, 1992.